Grain-size-dependent magnetic properties of nanocrystalline Gd

R. Kruk,[1,2] M. Ghafari,[3] H. Hahn,[1,3] D. Michels,[4] R. Birringer,[4] C. E. Krill III,[5] R. Kmiec,[2] and M. Marszalek[2]
[1]*Institute of Nanotechnology, Forschungszentrum Karlsruhe, D-76021 Karslruhe, Germany*
[2]*Institute of Nuclear Physics PAN, Radzikowskiego 152, 31-342 Krakow, Poland*
[3]*Joint Research Laboratory Nanomaterials Forschungszentrum Karlsruhe/Technische Universität Darmstadt, Institute of Materials Science, D-64287 Darmstadt, Germany*
[4]*FR. 7.3 Technical Physics, Universität des Saarlandes, Postfach 151150, Geb. 43, D-66041 Saarbrücken, Germany*
[5]*Materials Division, Universität Ulm, Albert-Einstein-Allee 47, D-89081 Ulm, Germany*
(Received 28 October 2005; revised manuscript received 3 January 2006; published 13 February 2006)

Microscopic magnetic and electronic properties of nanocrystalline Gd were studied by ^{155}Gd Mössbauer spectroscopy. This technique made it possible to distinguish the microstructure-dependent properties of Gd located in nanocrystal interiors from the properties of Gd in the grain boundaries. For the grain interiors a correlation between the induced magnetic anisotropy and the grain size was observed; this anisotropy can be attributed to the internal pressure resulting from the interface stress of the grain boundaries. The magnetic and electronic structure of the atoms in the grain boundaries differs distinctively from that in the grain interiors: the Gd magnetic moments at the grain boundaries are randomly oriented with respect to the local crystallographic axes, and the density of conduction *s* electrons is reduced, perhaps as a result of a lower number of Gd nearest neighbors.

DOI: 10.1103/PhysRevB.73.054420 PACS number(s): 75.50.Tt, 75.75.+a, 76.80.+y

I. INTRODUCTION

Bulk hexagonal Gd has been studied extensively in past decades and still attracts considerable experimental and theoretical attention, particularly concerning the electronic structure and fnite-temperature magnetic properties.[1–5] Experimentally, many of the ground-state properties of elemental Gd are well understood.[6–11] It crystallizes in the hcp structure with a lattice constant $a=0.3629$ nm and c/a ratio $=1.597$. Magnetic properties originate almost entirely from the half filled $4f$ shell ($L=0$, $J=S=7/2$), which contributes strictly localized magnetic moments. The zero-temperature moment μ $(T=0)=7.63\mu_B$ indicates that an induced polarization of the conduction bands of at least $0.63\mu_B$ arises from an interband exchange coupling (Ruderman-Kittel-Kasuya-Yosida type) between itinerant $5d/6s$ conduction-band electrons and the localized $4f$ electrons.[12,13] Gd is a ferromagnet with a Curie temperature $T_C=293$ K. Magnetization measurements,[6] neutron diffraction,[9] and crystalline anisotropy[14] show that the angle between the *c* axis and the easy axis of magnetization increases from around 32° at 10 K to around 65° at 183 K and drops abruptly to zero at $T\approx 232$ K. Using first-principles theory[15] it has recently been shown that the magnetic anisotropy energy (MAE) of Gd metal originates from classical dipole-dipole interactions between the large $4f$ spins (~ 7 μeV/atom) and from the MAE of the conduction electrons (16 μeV/atom). The latter contribution results from the spin-orbit splitting of the conduction electrons and is transferred to the $4f$ spin. The direction of the magnetic moment calculated for low temperature lies at an angle of 20° to the *c* axis, in good agreement with the experimental results.

Recent developments in the fields of magnetism and magnetic materials[16,17] have focused increasingly on nanostructures as a particularly interesting class of materials for both scientific and technological exploration. Current research is directed towards studying and understanding the influence of spatial confinement and order, topological arrangement, as well as the proximity of magnetic nanoscale building blocks (nanocrystals, nanorods, chains of nanocrystals, layers having a thickness of a few nm, etc.) on fundamental and applied magnetism. A key issue of fundamental research is devoted to understanding the effect of imperfections (defects) and structural disorder—which is present in any real nanostructured material—on extrinsic magnetic properties. So far, the overwhelming number of investigations of size-reduced systems with rare earth elements have been carried out on thin films and multilayer systems[18–23] or on clusters containing up to a few tens of atoms.[24,25] Studies of isolated or embedded nanocrystals or single or multicomponent bulk nanocrystalline materials are rare.[26–29] Nanocrystalline (nc) materials are thermodynamically unstable against grain growth, which takes place at elevated temperatures.[30] Consequently, annealing of as-prepared (kinetically frozen) nc specimens results in the evolution of microstructure toward the coarse-grained conventional polycrystalline state of a given material, which may in turn serve as a reference state. This latter feature enables nc materials to be model systems for the study of the influence of reduction in the structural correlation length (grain size) and the concomitant buildup of internal interface concentration on magnetic properties. Nanocrystalline Gd can be considered to be a polycrystal with randomly oriented nanometer-sized grains (the crystalline phase) embedded in a network of grain boundaries (GBs). It has recently been shown that in nanocrystalline Gd the fraction of GB atoms is sufficiently large to affect internal magnetic properties.[27] Therefore it is the aim of this study to investigate the effect of nanoscale polycrystallinity, as represented in nanocrystalline Gd, on the extrinsic magnetic and electronic properties of Gd. Mössbauer spectroscopy using the ^{155}Gd isotope provides a unique local probe

TABLE I. Parameters characterizing the specimen microstructure of coarse-grained and nanocrystalline (nc) Gd: area-weighted average crystallite size $\langle L\rangle_{area}$, the width of the *lognormal* crystallite size distribution σ,[a] microstrain e,[b] and the volume fraction (concentration) of GBs as obtained from $2\delta/\langle L\rangle_{area}$ where δ characterizes the structural width of the GB core region.

Sample	$\langle L\rangle_{area}$	σ	e	fraction of GBs
Reference sample	10 μm	/	/	2×10^{-4}
nc Gd	13 nm	1.7	0.24	0.15
nc Gd	8 nm	1.7	0.58	0.25

[a]Reference 32.
[b]Reference 31.

allowing the investigation of both the grain-boundary and crystalline components of nc Gd. Our studies were performed on representative nanocrystalline samples having average grain sizes of 8 and13 nm as well as on a coarse-grained 10-μm-sized reference sample.

II. EXPERIMENTAL DETAILS

Samples of nanocrystalline Gd were prepared by inert-gas condensation and subsequent compaction.[26] Pieces of Gd metal (99.99%) were evaporated in an ultrahigh-vacuum chamber (base pressure $\approx 10^{-8}$ mbar) filled with He gas to a pressure of 3 mbar. Nanometer-sized Gd clusters formed from the Gd vapor by condensation were collected on a liquid-nitrogen-cooled cold finger and subsequently compacted under high vacuum ($<10^{-7}$ mbar) at a pressure of about 1 GPa. The density of the resulting disk-shaped samples (8 mm diameter and 0.6 mm thickness) was determined by the Archimedes method to be approximately 99% of that of bulk Gd. Annealing of the nc specimens was carried out in sealed quartz tubes held at 700 °C for several hours. Prior to sealing, quartz tubes were preheated and repeatedly evacuated and filled with He inert gas (5.0 grade). Chemical analysis by hot-extraction gas chromatography found impurity levels of 0.1 at. % oxygen, 0.2 at. %, nitrogen, and 0.4 at. % hydrogen, whereas energy dispersive x-ray analysis revealed no evidence for heavy-element impurities.

X-ray diffraction was used to characterize the microstructure of the nanocrystalline Gd samples. Wide-angle diffraction scans were recorded on a Siemens D5000 diffractometer in θ-2θ geometry using Cu-$K\alpha$ radiation. From the background-corrected integral width of the Bragg peaks—as determined by full-pattern profile fitting—it is possible to determine the (area-weighted) average crystallite size $\langle L\rangle$ and the microstrain level e.[31,32] The volume fraction of GBs can then be calculated from the specific grain-boundary area A/V multiplied by the width of the GB core region, δ, whereby the stereological identity $A/V=2/\langle L\rangle$ relates the specific grain-boundary area to the average area-weighted grain size. Our results are summarized in Table I, assuming $\delta=1$ nm.

The ^{155}Gd Mössbauer studies of nc Gd were performed with a (^{155}Eu)$SmPd_3$ source and a standard constant-acceleration spectrometer of the Kankeleit type in transmission geometry was used. The velocity was calibrated during the measurements with a ^{57}Co(Rh) source and a metallic iron foil at room temperature. Spectra were recorded in a liquid-helium cryostat at 4.2 K.

III. DATA ANALYSIS

Understanding of the obtained Mössbauer spectra requires consideration of the full hyperfine interaction Hamiltonian. For a nuclear state with spin $\hat{I}$, the Hamiltonian represented in the principal-axis system of the electric-field-gradient tensor (EFG) assumes the form

$$\hat{H}=-g\mu_B H_{hf}\left[\hat{I}_z\cos\theta+\frac{1}{2}(\hat{I}_+e^{-i\varphi}+\hat{I}_-e^{i\varphi})\sin\theta\right]+\frac{\Delta E_Q}{4I(2I-1)}\left[3\hat{I}_z^2-\hat{I}^2+\frac{\eta}{2}(\hat{I}_+^2+\hat{I}_-^2)\right],$$

where the magnetic hyperfine field at the nuclear site is represented by H_{hf}; $\Delta E_Q=eV_{zz}Q$ is the quadrupole interaction constant, V_{zz} is the z component of the EFG tensor, and Q is the ground-state quadrupole moment of the ^{155}Gd nucleus; η is the asymmetry parameter defined as $\eta=(V_{xx}-V_{yy})/V_{zz}$; θ is the angle between the direction of H_{hf} and the V_{zz} axis; φ is the angle between the V_{xx} axis and the projection of the H_{hf} onto the xy plane. If the principal axes are chosen such that $|V_{xx}|<|V_{yy}|<|V_{zz}|$, then $0\leqslant\eta\leqslant1$. However, since the Gd site in the hexagonal hcp structure has a threefold symmetry axis, the value of the asymmetry parameter η is zero. Consequently, the shape of the spectra is independent of the angle φ. In order to obtain the positions of the resonance absorption lines, the eigenvalues and eigenfunctions of the Hamiltonian were numerically calculated for the ground ($I_g=3/2$) and excited ($I_{ex}=5/2$) states. The relative intensities of the resulting 24 resonance lines were calculated with the formulas given in Ref. 33. In addition to the hyperfine interaction Hamiltonian parameters, the isomer shift δ_{is} was determined. A transmission integral formula was applied to describe the resonance line shape, with the Debye-Waller factor f_A fitted as an independent parameter. The linewidth of the source Γ_S of 0.35 mm/s and the background corrected Debye-Waller factor f_S of the source were obtained from independent measurements with a standard $GdFe_2$ absorber. The gyromagnetic and quadrupole-moment ratios of ground and excited states were constrained to $g_{ex}/g_g=1.235$ and $Q_{ex}/Q_g=0.087$, respectively.[34] The interference factor ξ for the $E_\gamma=86.5$ keV gamma transition in the ^{155}Gd nuclei was set to $\xi=0.0275$.[35]

IV. EXPERIMENTAL RESULTS

The Mössbauer spectra (open circles) of three Gd samples with the area-weighted average crystallite sizes of 10 μm, 13 nm, and 8 nm are shown in Fig. 1. The full lines in Fig. 1 illustrate theoretical curves fitted to the experimental data by the least-squares method. All three spectra indicate that Gd is magnetically ordered. However, one can recognize at first glance differences between the spectra of the nanocrystalline

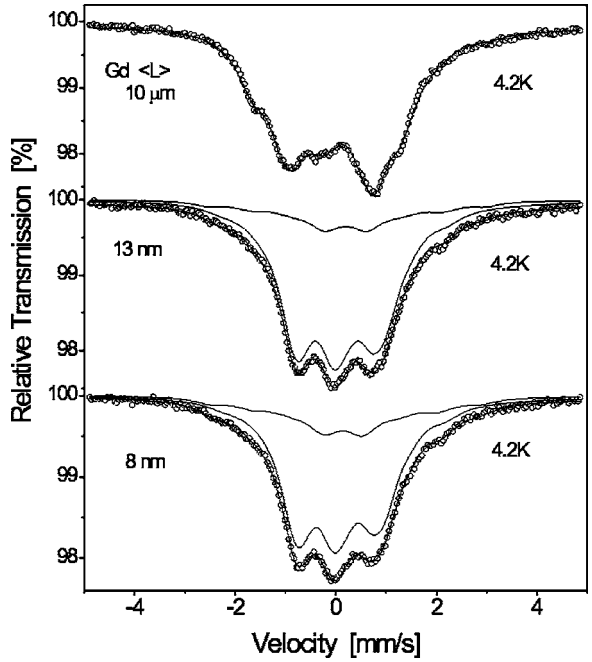

FIG. 1. ^{155}Gd Mössbaur spectra for the 10-μm reference sample and the nanocrystalline $\langle L\rangle$=13-nm, $\langle L\rangle$=8-nm samples. All spectra were collected at 4.2 K.

samples and that of the coarse-grained 10-μm reference sample. The reference spectrum with $\langle L\rangle$=10 μm resembles the Gd Mössbauer spectrum of a single crystal, while the nanocrystalline spectra reflect features of typical powder spectra.[36] This observation suggests the presence of a strong preferred orientation of the crystallographic c axis with respect to the direction of gamma radiation in the reference absorber and a random grain orientation distribution in the nanocrystalline specimens. In order to fit the spectra of the reference sample, it was necessary to set a preferred orientation angle of about 30° between the crystallographic c axis and the direction of gamma radiation (Fig. 2). As a result, the reference spectrum can be described unambiguously with a single set of hyperfine parameters (one-component fit). It is noteworthy that the computed hyperfine parameters are similar to the respective single-crystal values (see Table II and Ref. 36). On the other hand, the nc samples yield no evidence of preferred orientation. Furthermore, every attempt to describe the nc spectra with a single-component fit was unsuccessful. However, all features of the spectra could be reproduced, particularly those at the shoulders of the spectra (Fig. 1), assuming the presence of two structurally different environments of the absorber in nc Gd. In the case of the second, low intensity, component the local symmetry of the Gd sites is unknown, thus the asymmetry parameter η is not necessarily zero. Unfortunately, the asymmetry parameter and quadrupole constant are strongly correlated which makes it very difficult to obtain their values separately. Therefore instead of fitting them independently, we used one effective parameter ΔE_Q^{eff} as a realistic approximation. The derived Mössbauer parameters and the relative intensities of the components are given in Table II. The Mössbauer parameters (H_{hf}, ΔE_Q, δ_{is}) of the dominant components are similar to the values obtained for Gd powders[36] (Table II). We note that the spectrum of the $\langle L\rangle$=13-nm sample is more symmetric than that of the $\langle L\rangle$=8-nm specimen (Fig. 1). This difference is due to the angle θ of the dominant components, which for the 8-nm sample takes on just one well-defined value, while for the $\langle L\rangle$=13-nm sample it was necessary to assume the existence of two angles (see Table II).

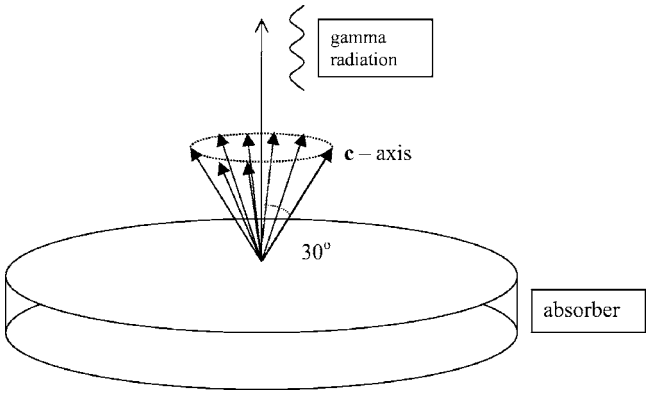

FIG. 2. The geometry of the experimental setup and the preferred orientation determined for the reference 10-μm compacted powder.

TABLE II. Mössbauer parameters at 4.2 K for the Gd nanocrystallites. H_{hf} represents the hyperfine field, θ is the angle between V_{zz} axis of the EFG tensor and H_{hf}, δ_{is} is the isomer shift, ΔE_Q is the quadrupole splitting constant, ΔE_Q^{eff} is the effective parameter for the second component (see text), RA_k is the relative intensity for the k component.

Compound	Components	H_{hf} (kOe)	θ (deg)	δ_{is} (mm/s)	ΔE_Q, ΔE_Q^{eff} (mm/s)	RA_k [%]
Gd, 8 nm	1	328(2)	73(1)	0.029(3)	1.52(8)	79
	2	356(6)	53(2)	0.17(2)	4.2(1)	21
Gd, 13 nm	1	332(2)	27;73	0.034(4)	1.52(8)	11;73
	2	362(9)	52(2)	0.24(3)	4.2(2)	16
Gd, 10 μm		361(2)	27(2)	0.025(3)	1.65(6)	
Single crystal[a]		373(5)	28(2)		1.52(5)	
Powder[a]		327(5)	75(3)		1.6(2)	

[a]Reference 36.

V. DISCUSSION

In order to interpret the Mössbauer hyperfine parameters in terms of the magnetic properties of nc Gd, we refer to a relationship between the hyperfine field at the Gd nuclei and the magnetic moment of Gd. The effective magnetic hyperfine field $\hat{H}_{hf}$ can be expressed as the sum of two terms:

$$\hat{H}_{hf} = \hat{H}_{cp} + \hat{H}_{ce}.$$

The core polarization field $\hat{H}_{cp}$ represents a contribution due to the exchange interaction between the local 4f electrons

and the core electrons. Its value, −340 kOe,[37] is usually assumed to be insensitive to the environment of the Gd atoms in the solid state. The negative sign arises from the fact that $\hat{H}_{cp}$ is directed opposite to the Gd magnetic moment. The conduction electron polarization term $\hat{H}_{ce}$ is ascribed to the polarization of conduction electrons by the parent ion and the nearest-neighbor Gd spins. With a good approximation both $\hat{H}_{cp}$ and $\hat{H}_{ce}$ contributions are aligned parallel to the Gd magnetic moment. Based on this orientation relationship, it is straightforward to determine the direction of the Gd magnetic moment with respect to the crystallographic axes. The unit cell of Gd metal contains just one Gd crystallographic site. One of the local symmetry elements at the Gd site is the threefold symmetry axis parallel to the crystallographic *c* axis. As a consequence, the V_{zz} axis of the EFG tensor is oriented parallel to the *c* axis and the two remaining components of the EFG tensor lie in the *ab*-basal plane (Fig. 3). Therefore the angle θ obtained by the fit procedure is directly related to the angle between the Gd magnetic moment and the *c* axis. This assertion is supported by the fact that the angle θ of 27(2)° derived from the Mössbauer spectrum of the reference sample is in a very good agreement with the value of about 32° obtained from neutron-diffraction experiments on a Gd single crystal.[9] Overall, the reference sample behaves almost like the Gd single crystals investigated with magnetometry, neutron-diffraction, and Mössbauer spectroscopy.[6,9,36] Consequently, our notion that coarse-grained polycrystalline samples may serve as reference samples, reflecting essentially the behavior of an undisturbed crystal lattice, is strongly corroborated by this finding.

Analysis of the measured Mössbauer spectra of the nc samples yields two sorts of subspectra: (i) dominant components having high intensity and hyperfine parameters consistent with a hcp crystal environment of the absorber, and (ii) an additional component of low intensity, which we attribute to the absorbing nuclei being located in the core region of GBs. In the following discussion, we refer to these two quantities as the crystalline and the GB component, respectively, suggesting that nc specimens of Gd, despite the presence of but a single chemical component, manifest the existence of two structurally distinct phases. This conjecture is supported by the fact that the relative area ratios of the component signals are roughly proportional to the volume fractions of Gd ions located in the GB core regions (Table I).

A comparison of the crystalline components of each sample reveals that the angle θ begins to deviate with decreasing grain size from the coarse grained reference value of 27° and finally assumes a value of 73° for the $\langle L\rangle$=8-nm specimen [Figs 3(a)–3(c)]. A presence of two angles θ for the crystalline component was a prerequisite to fitting the measured data of the $\langle L\rangle$=13-nm specimen [Fig. 3(b)]. We interpret this outcome as an indication of the existence of a crossover state in which a discontinuous transition between the two single-valued θ angles takes place. In other words, the rotation of the magnetic moment toward the basal plane in nc Gd suggests a modification of and/or an additional contribution to the magnetic anisotropy energy (MAE). As recently pointed out,[15] the MAE originates in the dipole-dipole interaction between the 4*f* spins and the MAE

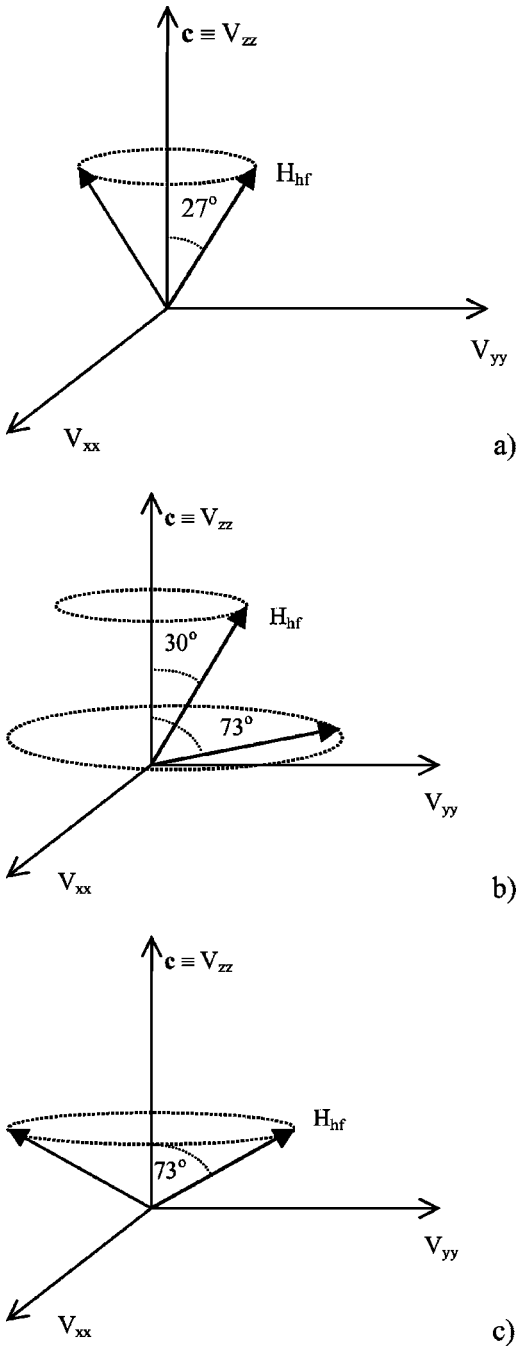

FIG. 3. The derived arrangement of the Gd magnetic moments in the grains for (a) reference 10-μm powder, (b) 13-nm nanocrystallites, and (c) 8-nm crystallites.

of the conduction electrons, which is extremely sensitive to the band fine structure close to the Fermi surface. In fact, this idea had been put forward by Franse *et al.*[38] in order to interpret magnetic torque measurements on a Gd single crystal at 4 K as a function of applied hydrostatic pressure. Although the maximum pressure available in this experiment was only 0.6 GPa, a strongly pressure-dependent magnetic anisotropy was observed. As a matter of fact, at an applied pressure of 0.6 GPa a second minimum in the MAE appears above an angle of 60°. Therefore it seems evident that the

angle θ of 73° observed in nc Gd at grain sizes near 8 nm has some connection to the pressure.

Michels *et al.*[27] suggested that the grain-size-dependent Curie transition in nc Gd may have its root in the interface stress, arising from the fact that the mere presence of GBs induces an internal hydrostatic pressure $\Delta p_{\mathrm{int}} \approx (2/3)\langle f \rangle A/V$, where $\langle f \rangle$ denotes the area-weighted isotropic interface stress of the GBs.[39,40] Typically, $\langle f \rangle$ is on the order of one to several N/m; as a consequence, the pressure exerted on 13 nm-sized nanocrystallites by the grain boundaries is on the order of 1 GPa, as such supporting our notion of a pressure-induced rotation of the magnetic moment toward the basal plane. A second source of magnetic anisotropy enters into the problem through the presence of microstrain e, which is a measure of rather short-ranged fluctuations in the spacing of lattice planes in the interior regions of the nanocrystallites. Such fluctuations could give rise to deviations from the pure S state of the Gd ion through crystal-field effects, resulting in additional magnetic anisotropy; likewise, magnetoelastic coupling may also contribute to MAE.

Another feature related to the grain size is the decrease of the effective hyperfine field H_{hf} with increasing θ (see Table I). Since the value of H_{cp} is unaffected by microstructure or pressure, it should be identical in all samples; therefore any variations in H_{hf} must be caused by a polarization of conduction electrons, which would be reflected in a change in the value of H_{ce}. Specifically, H_{ce} changes sign from negative in the nc state to positive in the coarse-grained reference state. Overall, this behavior lends additional support to the idea that the spin-orbit splitting of the conduction electrons and the high sensitivity of the density of states in the near vicinity of the Fermi energy to pressure are the main origin of magnetic anisotropy in nc Gd.

Last, we discuss the isomer shift and quadrupole splitting in the crystalline and GB components (Table II). The isomer shift is proportional to the density of *s* electrons at the nucleus site and is sensitive to the character of chemical bonding of Gd. For Gd the isomer shift tends to be increasingly positive with a decreasing density of *s* electrons. The smaller value of the isomer shift of Gd in the crystalline component ($\delta_{\mathrm{is}}=0.029$ mm/s) compared to that of the GB component ($\delta_{\mathrm{is}}=0.17$ mm/s) indicates a lower *s* electron density in the core region of GBs than in the grain interiors. This difference may be a consequence of a reduced number of Gd nearest neighbors and an altered atomic arrangement in the GB cores. The decrease in *s* electron density at GBs is, to some extent, corroborated by the electron structure calculations of free-standing Gd thin films.[1] These calculations show that in ferromagnetically ordered Gd the surface layer has a lower density of 6*s* electrons than in bulk Gd. The structural difference between the interior regions of nanocrystals and the GB cores is also reflected in a quadrupole splitting that is almost three times larger in the GBs than in the regular hcp crystalline environment. This may be indicative of a lower local symmetry of the Gd sites in the GBs. The angle θ of about 53° derived for the GB component is close to the angle of 54.7° that one can get by averaging over all directions of magnetic moments with respect to the local crystallographic axes. This particular angle may be a sign of a random distribution of magnetic moments with respect to the main axes of the EFG tensor. In fact, it is plausible to expect a random arrangement of Gd magnetic moments with respect to the local V_{zz} axes at GBs, as it is likely that the Gd moments at GBs are subjected to competing magnetic interactions originating in the adjacent grains. Moreover, local crystallographic disorder at GBs could also contribute to a random distribution of Gd magnetic moments in the GB core regions.

VI. CONCLUSIONS

Microscopic magnetic and electronic properties of nanocrystalline Gd bulk samples were studied by the technique of ^{155}Gd Mössbauer effect spectroscopy. The resonance spectra allowed discrimination of the signals arising from Gd absorbers located in the core regions of grain boundaries from those arising from absorbers in the nanocrystal interiors. From the hyperfine parameters obtained in this manner, we were able to determine microstructure dependence of several magnetic properties.

(i) A correlation between the average grain size and induced strong magnetic anisotropy in the crystalline component was found. At some critical grain size the Gd magnetic moments change abruptly their direction from an angle of 20° characteristic of the course-grained sample to 73° for the nanocrystalline samples. The magnetic anisotropy driving this rotation could be attributed to the compressive stress (pressure) that is induced in the crystalline component by the interface stress of the grain boundaries.

(ii) The magnetic and electronic structure of the grain-boundary core regions were found to differ significantly from those of the nanocrystal interiors. The Gd magnetic moments in the core area of grain boundaries are randomly oriented with respect to their local crystallographic axes. A reduced number of Gd nearest neighbors, bond disorder, weakened and/or broken bonds at the grain boundaries are indicated by the reduced density of conduction *s* electrons and the large quadrupole splitting.

[1] R. Wu, C. Li, A. J. Freeman, and C. L. Fu, Phys. Rev. B **44**, 9400 (1991).
[2] B. N. Harmon and A. J. Freeman, Phys. Rev. B **10**, 1979 (1974).
[3] M. Richter and H. Eschrig, Solid State Commun. **72**, 263 (1989).
[4] P. Kurz, G. Bihlmayer, and S. Blügel, J. Phys.: Condens. Matter **14**, 6353 (2002).
[5] C. Santos, W. Nolting, and V. Eyert, Phys. Rev. B **69**, 214412 (2004).
[6] H. E. Nigh, S. Legvold, and F. H. Spedding, Phys. Rev. **132**, 1092 (1963).

[7] F. J. Darnell, Phys. Rev. **130**, 1825 (1963).
[8] R. J. Elliot, in *Magnetism*, edited by G. T. Rado and H. Suhl (Academic Press, New York, 1965), Vol. II, part A, pp. 385–425.
[9] J. W. Cable and E. O. Wollan, Phys. Rev. **165**, 733 (1968).
[10] B. Coqblin, *The Electronic Structure of Rare-Earth Metals and Alloys: The Magnetic Heavy Rare-Earth* (Academic Press, London, 1977).
[11] J. Jensen and A. R. Makintosh, *Rare Earth Magnetism* (Clarendon, Oxford, 1991).
[12] T. Kasuya, Prog. Theor. Phys. **16**, 45 (1956).
[13] K. Yosida, Phys. Rev. **106**, 893 (1957).
[14] F. Milstein and L. B. Robinson, Phys. Rev. **177**, 904 (1969).
[15] M. Colarieti-Tosti, S. I. Simak, R. Ahuja, L. Nordström, O. Eriksson, D. Aberg, S. Edvardsson, and M. S. S. Brooks, Phys. Rev. Lett. **91**, 157201 (2003).
[16] R. Skomski, J. Phys.: Condens. Matter **15**, R841 (2003).
[17] M. R. Fitzsimmons, S. D. Bader, J. A. Borchers, G. P. Felcher, J. K. Furdyna, A. Hoffmann, J. B. Kortright, I. K. Schuller, T. C. Schulthess, S. K. Sinha, M. F. Toney, D. Weller, and S. Wolf, J. Magn. Magn. Mater. **271**, 103 (2004).
[18] M. Farle, K. Baberschke, U. Stetter, A. Aspelmeier, and F. Gerhardter, Phys. Rev. B **47**, R11571 (1993).
[19] E. D. Tober, R. X. Ynzunza, C. Westphal, and C. S. Fadley, Phys. Rev. B **53**, 5444 (1996).
[20] M. Gajdzik, T. Trappmann, C. Sürgers, and H. v. Löhneysen, Phys. Rev. B **57**, 3525 (1998).
[21] M. E. Fisher and A. E. Ferdinand, Phys. Rev. Lett. **19**, 169 (1967).
[22] C. Domb, J. Phys. A **6**, 1298 (1973).
[23] M. Przybylski and U. Gradmann, Phys. Rev. Lett. **59**, 1152 (1987).
[24] D. C. Douglass, J. P. Bucher, and L. A. Bloomfield, Phys. Rev. Lett. **68**, 1774 (1992).
[25] D. Gerion, A. Hirt, and A. Chătelain, Phys. Rev. Lett. **83**, 532 (1999).
[26] C. E. Krill, F. Merzoug, W. Krauss, and R. Birringer, Nanostruct. Mater. **9**, 455 (1997).
[27] D. Michels and C. E. Krill, R. Birringer, J. Magn. Magn. Mater. **250**, 203 (2002).
[28] J. Weissmüller, A. Michels, D. Michels, A. Wiedenmann, C. E. Krill III, H. M. Sauer, and R. Birringer, Phys. Rev. B **69**, 054402 (2004).
[29] Z. C. Yan, Y. H. Huang, Y. Zhang, H. Okumura, J. Q. Xiao, S. Stoyanov, V. Skumryev, G. C. Hadjipanayis, and C. Nelson, Phys. Rev. B **67**, 054403 (2003).
[30] C. E. Krill III, L. Helfen, D. Michels, H. Natter, A. Fitch, O. Masson, and R. Birringer, Phys. Rev. Lett. **86**, 842 (2001).
[31] C. E. Krill, R. Haberkorn, and R. Birringer, in *Handbook of Nanostructured Materials and Nanotechnology*, edited by H. S. Nalwa (Academic Press, San Diego, 2000), Vol. 2, Chap. 3, pp. 155–211.
[32] C. E. Krill and R. Birringer, Philos. Mag. A **77**, 621 (1998).
[33] D. P. Pappas, A. P. Popov, A. N. Anisimov, B. V. Reddy, and S. N. Khanna, Phys. Rev. Lett. **76**, 4332 (1996).
[34] H. Armon, E. R. Bauminger, and S. Ofer, Phys. Lett. **43B**, 380 (1973).
[35] K. Tomala, G. Czjzek, J. Fink, and H. Schmidt, Solid State Commun. **24**, 857 (1977).
[36] E. R. Bauminger, A. Diamant, I. Felner, I. Nowik, and S. Ofer, Phys. Rev. Lett. **34**, 962 (1975).
[37] Le Dang Khoi, Phys. Lett. **28A**, 671 (1969).
[38] J. J. M. Franse and R. Gersdorf, Phys. Rev. Lett. **45**, 50 (1980).
[39] J. Weissmüller and J. W. Cahn, Acta Mater. **45**, 1899 (1999).
[40] R. Birringer, M. Hoffmann, and P. Zimmer, Z. Metallkd. **94**, 1052 (2003).